Peripheral Nerve Involvement in Multiple Sclerosis: Demonstration by Magnetic Resonance Neurography

Johann M. E. Jende, MD,[1]* Gesa H. Hauck, MD,[1,2]* Ricarda Diem, MD,[3]
Markus Weiler, MD,[3] Sabine Heiland, PhD,[1,4] Brigitte Wildemann, MD,[3]
Mirjam Korporal-Kuhnke, MD,[3] Wolfgang Wick, MD,[3] John M. Hayes, BA,[5]
Johannes Pfaff, MD ![ORCID],[1] Mirko Pham, MD,[1,6] Martin Bendszus, MD,[1] and
Jennifer Kollmer, MD[1]

Objective: To detect and quantify peripheral nerve lesions in multiple sclerosis (MS) by magnetic resonance neurography (MRN).

Methods: Thirty-six patients diagnosed with MS based on the 2010 McDonald criteria (34 with the relapsing–remitting form, 2 with clinically isolated syndrome) with and without disease-modifying treatment were compared to 35 healthy age-/sex-matched volunteers. All patients underwent detailed neurological and electrophysiological examinations. Three Tesla MRN with large anatomical coverage of both legs and the lumbosacral plexus was performed by using 2-dimensional (2D) fat-saturated, T2-weighted (T2w) and dual echo turbo spin echo sequences as well as a 3D T2-weighted, fat-saturated SPACE sequence. Besides qualitative visual nerve assessment, a T2w signal quantification was performed by calculation of proton spin density and T2 relaxation time. Nerve diameter was measured as a morphometric criterion.

Results: T2w hyperintense nerve lesions were detectable in all MS patients, with a mean lesion number at thigh level of 151.5 ± 5.7 versus 19.1 ± 2.4 in controls ($p < 0.0001$). Nerve proton spin density was higher in MS (tibial/peroneal: $371.8 \pm 7.7/368.9 \pm 8.2$) versus controls (tibial/peroneal: $266.0 \pm 11.0/276.8 \pm 9.7$, $p < 0.0001$). In contrast, T2 relaxation time was significantly higher in controls (tibial/peroneal: $82.0 \pm 2.1/78.3 \pm 1.7$) versus MS (tibial/peroneal: $64.3 \pm 1.0/61.2 \pm 0.9$, $p < 0.0001$). Proximal tibial and peroneal nerve caliber was higher in MS (tibial: $52.4 \pm 2.1\,mm^2$, peroneal: $25.4 \pm 1.3\,mm^2$) versus controls (tibial: $45.2 \pm 1.4\,mm^2$, $p < 0.0015$; peroneal: $21.3 \pm 0.7\,mm^2$, $p = 0.0049$).

Interpretation: Peripheral nerve lesions could be visualized and quantified in MS in vivo by high-resolution MRN. Lesions are defined by an increase of proton spin density and a decrease of T2 relaxation time, indicating changes in the microstructural organization of the extracellular matrix in peripheral nerve tissue in MS. By showing involvement of the peripheral nervous system in MS, this proof-of-concept study may offer new insights into the pathophysiology and treatment of MS.

ANN NEUROL 2017;82:676–685

M ultiple sclerosis (MS), one of the most common acquired chronic neurological diseases, is traditionally regarded as restricted to the central nervous system (CNS), but the exact etiology is still unclear. With an estimated prevalence of 2 million affected people worldwide, it is one of the leading causes of disability in young adults.[1] The clinical presentation of MS is heterogeneous, with sensory, motor, visual, and autonomic symptoms.

Clinically, MS is diagnosed based on the principles of symptom dissemination in space and time as defined by the Poser criteria.[2] According to the 2010 McDonald criteria, the early diagnosis of MS after a single clinical event can be established by the radiological demonstration of lesion dissemination in space and time.[3]

A few studies, most of them case reports, suggest the concurrence of demyelination in the CNS and peripheral nervous system (PNS) in MS. Earlier neuropathological reports described segmental demyelination, hypertrophic neuropathy, and reduction in myelin thickness in a few MS patients.[4,5] Large electrophysiological studies of nerve conduction abnormalities in MS are rare, and documented results are inhomogeneous regarding type, frequency, and extent of PNS involvement.[6,7]

High-resolution magnetic resonance neurography (MRN) enables early detection and precise localization of peripheral nerve lesions with high sensitivity, down to the level of nerve fascicles in various neuropathies, and thus can overcome typical diagnostic limitations of nerve conduction studies (NCS).[8,9] With an extensive MRN imaging protocol and in correlation with NCS, we (1) tested the involvement of the PNS in MS; (2) analyzed peripheral nerve lesions by in vivo visualization, localization, and T2-weighted (T2w) signal quantification; and (3) compared MRN findings of healthy volunteers to those of MS patients in correlation with the presence of spinal cord lesions.

Subjects and Methods

Study Design and Patients

The local ethics committee approved this study (University of Heidelberg S-405/2012; J.P., M.B.), and all participants gave written informed consent. Thirty-six MS patients (21 female, 15 male, mean age = 32.1 years, range = 18–43, 2010 McDonald criteria fulfilled in all patients) with either relapsing–remitting MS (>3 years, range = 3–13, n = 34) or clinically isolated syndrome (n = 2) and 35 sex- and age-matched healthy volunteers (19 female, 16 male, mean age = 31.6, range = 22–40) were included in this prospective, cross-sectional, single center study between May 2015 and September 2016. Current gadolinium-enhanced magnetic resonance imaging (MRI) studies of the brain and spine were available in all patients with MS. The mean time gap between the acquisition of the MRN scans and the most recent available CNS MRI was 1.5 ± 0.3 months (median = 1 month) for imaging of the brain and 5.5 ± 1.3 months (median = 3 months) for imaging of the spinal cord. Overall exclusion criteria were age < 18 or > 45; pregnancy; any contraindications for MRI; any risk factors for neuropathy such as diabetes mellitus, alcoholism, and malignant or infectious diseases; any therapy with steroids in the 8 weeks immediately prior to the MRI scans; and any previous exposure to neurotoxic agents. Additionally, by taking a detailed past medical history, any sensory or motor symptoms in the upper or lower extremities, any history of neuropathy, any previous spine surgery, and any permanent medication was ruled out in all healthy volunteers.

Clinical and Electrophysiological Examination

A detailed medical history was documented for each patient, and a comprehensive neurological examination (R.D., B.W., M.K.-K.) was performed, including evaluation of the Expanded Disability Status Scale (EDSS).[10] NCS of the left leg included distal motor latencies, compound muscle action potentials, and F-waves of the tibial and peroneal nerves; nerve conduction velocities of the tibial, peroneal, and sural nerves; and sensory nerve action potentials of the sural nerve (M.W.). Skin temperature was controlled at a minimum of 32 °C. Detailed clinical and electrophysiological data are presented in Supplementary Tables 1 and 2.

MRN Protocol

All participants underwent high-resolution MRN in a 3.0T magnetic resonance scanner (Magnetom TIM-TRIO, Siemens Healthcare, Erlangen, Germany):

1. Three-dimensional (3D) T2-weighted inversion recovery SPACE (Sampling Perfection with Application-optimized Contrasts using different flip angle Evolution) sequence for imaging of the lumbar plexus and spinal nerves with 50 axial reformations/patient: repetition time = 3,000 milliseconds, effective echo time = 62 milliseconds, inversion time = 210 milliseconds, field of view = $305 \times 305mm^2$, matrix size = $320 \times 320 \times 104$, slice thickness = 1.0mm, no gap, voxel size = $1.0 \times 1.0 \times 1.0mm^3$, acquisition time 8 minutes 32 seconds.

2. Axial high-resolution T2-weighted turbo spin echo two-dimensional (2D) sequences with spectral fat saturation (3 slabs at the right leg). Slab 1: proximal thigh to midthigh; slab 2: lower leg with alignment of its proximal edge with the tibiofemoral joint space; slab 3: ankle level with alignment of the distal edge of the imaging slab on the tibiotalar joint space. Repetition time = 5,970 milliseconds, echo time = 55 milliseconds, field of view = $150 \times 150mm^2$, matrix size = 512×512, slice thickness = 3.5mm, interslice gap = 0.35mm, voxel size = $0.4 \times 0.3 \times 3.5mm^3$, 35 slices, acquisition time per slab = 4 minutes 42 seconds.

3. Axial high-resolution dual echo turbo spin echo 2D-sequence with spectral fat saturation (1 slab per leg, equaling 2 slabs per subject): midthigh to distal thigh with alignment of the distal edge of this imaging slab on the tibiofemoral joint space. Repetition time = 5,210 milliseconds, echo time$_1$ = 12 milliseconds, echo time$_2$ = 73 milliseconds, field of view = $150 \times 150mm^2$, matrix size = 512×512, slice thickness = 3.5mm, interslice gap = 0.35mm, voxel size = $0.4 \times 0.3 \times 3.5mm^3$, 35 slices, acquisition time per slab = 7 minutes 30 seconds.

Net imaging time including survey scans was 38 minutes 2 seconds. Patient and coil repositioning required additional time, resulting in a total examination time of 60 to 70 minutes

per participant. A 4-channel body-array flex-coil (Siemens Healthcare, Erlangen, Germany) was used for imaging of the lumbar plexus (sequence 1), and a 15-channel transmit-receive extremity-coil (Invivo, Gainesville, FL) for imaging of the right and left leg (sequences 2 and 3, respectively). All coils used in this study are commercially available.

Image Postprocessing and Statistical Analysis

All images generated by MRI sequences 2 and 3 were pseudonymized (M.B., J.P.) and subsequently analyzed in FSL, a dedicated software for neuroimaging data evaluation.[11] Tibial and peroneal fascicles of the sciatic nerve and their distal continuation as either tibial or peroneal nerve were manually segmented by one neuroradiologist (G.H.H.) from proximal thigh down to distal ankle level on 140 axial slices for the left leg, and only at thigh level on an additional 35 slices for the right leg. The contour between nerve fascicles and the epineurium was used as a reliably visible segmentation border. Slice numbering for the tibial nerve was from 0 (most proximal slice at proximal thigh level) to 139 (most distal slice at ankle level) and from 0 to 60 (level of the fibular head) for the peroneal nerve. For simplification, we refer to tibial fascicles of the sciatic nerve and corresponding tibial nerve as tibial nerve only, and to peroneal fascicles of the sciatic nerve and corresponding common peroneal nerve as peroneal nerve.

Qualitative Evaluation of Nerve Lesions

Based on the 2010 McDonald criteria, the evaluation of T2w hyperintense lesions in the brain and spinal cord is an established method in the initial diagnostic workup of patients with MS, as well as in their lifelong radiological follow-up. According to this standard procedure, 2 experienced, independent neuroradiologists (J.M.E.J., J.K.), who were blinded to clinical data, performed a visual evaluation and determination of the total sciatic nerve lesion count on 20 representative axial imaging slices at left proximal thigh level. We defined a nerve lesion as a nerve fascicle with an abnormally high T2w signal. Lesion number per slice position was counted and then summed to a total lesion number within the imaged volume per participant. Subsequently, mean values were calculated over all participants within either the MS or the control group.

Recent spinal cord MRIs of all MS patients were additionally analyzed to exclude potential external sources of nerve affection such as spinal cord or nerve root compression due to herniated vertebral disks or spinal tumors. Once external reasons for nerve damage were ruled out, the total number of T2w hyperintense lesions to the spinal cord was evaluated. The total number of spinal cord lesions was then correlated with the total number of sciatic nerve lesions at thigh level.

Tibial and Peroneal Nerve T2w Signal

In previous studies on nerve lesion detection and quantification in 2 different polyneuropathies,[12,13] we performed an extensive histogram-based normalization of nerve T2w signal intensities and a fully automatic and operator-independent binary classification of respective tibial and peroneal nerve voxels as either nerve lesion voxels or nonlesion voxels. With this method, we have already proven that an increase of nerve T2w signal reflects true nerve lesions.[12,13] To facilitate statistical evaluations, we analyzed nerve T2w signal without any further signal normalization in the current study.

Mean nerve T2w signal was calculated per slice position for each subject and for each left leg. To receive detailed information about the anatomical distribution of nerve lesions and thereby information about the location of predominant nerve affection, we compared mean tibial nerve T2w signals of 35 slices at proximal to midthigh level (slice positions 0–35) to their distal equivalent of 35 slices at the lower leg (proximal to middle part; slice positions 70–105). The peroneal nerve was evaluated from proximal to midthigh level (slice positions 0–35) only. Averaged mean values within all proximal slices were statistically compared between the 2 groups (MS vs controls) by using the Mann–Whitney test; additional mean values within all distal slices were evaluated for the tibial nerve only.

Nerve Lesion Quantification: Apparent T2 Relaxation Time and Proton Spin Density

Quantification of nerve lesions was performed by calculating the apparent T2 relaxation time ($T2_{app}$, Eq 1) and proton spin density (ρ, Eq 2), by the following formulas[14]:

$$T2_{app} = \frac{TE_2 - TE_1}{\ln\left(SI(TE_1)/SI(TE_2)\right)} \qquad (1)$$

$$\rho = \frac{SI(TE_1)}{\exp(-TE_1/T2_{app})} \qquad (2)$$

As indicated by the 2 formulas, calculation of $T2_{app}$ and ρ required the acquisition of an additional pulse sequence at 2 different echo times (sequence 3 with echo $time_1 = 12$ milliseconds and echo $time_2 = 73$ milliseconds). To hold a reasonable total acquisition time, the dual echo sequence was acquired at thigh level only. That was done in accordance with previous studies in different neuropathies, where we have already proven their feasibility of application in the PNS, and their high sensitivity for early nerve lesion detection.[12,13]

Morphometric Quantification: Nerve Diameter

Nerve caliber was analyzed by measuring the complete cross-sectional area of the tibial and peroneal nerve on each axial slice. Two-way analysis of variance (ANOVA) was performed to test group differences (MS vs controls) and differences between anatomical regions (proximal slice positions 0–69 vs distal slice positions 70–139). Peroneal nerve caliber was analyzed from proximal thigh level down to the level of the fibular head only (slice positions 0–60).

Lumbosacral Plexus and Spinal Nerves

Bilateral dorsal root ganglia and corresponding proximal spinal nerves L5 and S1 were segmented on axial reformations of sequence 1 by manually delineating the nerve circumference as the intraneural region of interest. In the same manner, the

lumbosacral plexus was segmented at the level of the sciatic notch on both sides. Subsequently, signal ratios between intraneural regions of interest and ipsilateral psoas (L5 and S1) or piriformis muscle (plexus) were calculated. Additional quantification of spinal nerve and plexus caliber was performed by measuring the cross-sectional area of the corresponding nerve on each axial slice.

Statistical Analysis

Statistical data analysis was performed with GraphPad (La Jolla, CA) Prism 6 (J.K., J.M.H.). Differences between MS patients and controls were evaluated with the Mann–Whitney test. Where appropriate, a 1-way or 2-way ANOVA was used for a priori assumptions, and subsequent post hoc comparisons were evaluated with the Fisher test. Statistical tests were 2-tailed, and an alpha level of significance was defined at $p < 0.05$. All results are documented as mean values $\pm$ standard error of the mean.

Results

Clinical and Electrophysiological Data

There was no significant difference between MS patients and controls for age, sex, body weight, and height (Table). In MS patients, the mean overall EDSS score was 2.0 ± 0.3. Thirty-one patients received disease-modifying medical treatment (EDSS 2.0 ± 0.3), whereas 5 patients had been free of immunomodulating medical treatment during the course of their disease (EDSS 2.1 ± 0.9). All patients fulfilled the revised 2010 McDonald criteria (see Supplementary Table 1). Electrophysiological findings were normal with the exception of 3 patients having marginally amplitude-reduced sural sensory nerve action potentials (Patients 11, 13, and 15), 1 patient having nonelicitable F waves of the peroneal nerve (Patient 23), and another with nonelicitable F waves of the tibial and peroneal nerves (Patient 15) in otherwise normal electroneurographic parameters and without clinical evidence of peripheral nerve dysfunction (see Supplementary Table 2). Moreover, there was no evidence for metabolic or vasculitic neuropathy in CSF or blood tests (eg, metabolic panel, vitamin B12) at the time of diagnosis. Lumbar MRI ruled out concurrent nerve root compression.

Qualitative Evaluation of Nerve Lesions

Qualitative visual evaluation revealed marked T2w hyperintense nerve lesions in all MS patients independent of their prior medication and with a mean lesion number at thigh level of 152.7 ± 4.1 versus 19.3 ± 1.7 in controls ($p < 0.0001$). Further subgroup analyses between treated MS patients versus controls and also between untreated MS patients versus controls revealed high differences for both groups ($p < 0.0001$; Figs 1 and 2), whereas differences between treated and untreated MS patients were not significant ($p = 0.64$). Calculated Cohen kappa was 1.000 for interobserver reliability to visually classify all participants into either MS or non-MS. High interobserver reliability was also found for the subsequent evaluation of the sciatic nerve lesion count (lesion number), with Pearson r of 0.9978 (control group) and 0.9892 (MS group). Fascicular lesions in all MS patients showed a diffuse distribution pattern, with a median length of 7.35mm, not involving fascicular segments longer than 11.2mm.

The additional evaluation of spinal cord T2w lesions in MS patients revealed a strong negative correlation between spinal cord lesions and sciatic nerve lesions ($r = -0.51$, $p = 0.002$). In all MS patients, we found no spinal cord T2w lesions below L1 and no signs of spinal cord or nerve root compression.

Proton Spin Density

The Mann–Whitney test revealed higher ρ in MS patients (tibial nerve: 371.8 ± 7.7 arbitrary units [a.u.], peroneal nerve: 368.9 ± 8.2 a.u.) versus healthy controls (tibial nerve: 266.0 ± 11.0 a.u., peroneal nerve: 276.8 ± 9.7 a.u., $p < 0.0001$ for both nerves; Figure 3).

As ρ was found to be the parameter with highest sensitivity for detecting PNS affection in MS patients, and to rule out that an increase of ρ was not related to the appearance of spinal cord lesions, we evaluated ρ in subgroups of MS patients with and without spinal cord lesions. One-way ANOVA revealed marked differences between the 3 groups (MS patients with spinal cord lesions vs MS patients without spinal cord lesions vs controls) with $p < 0.0001$. Post hoc comparisons showed significant differences of mean tibial nerve ρ between controls (26.0 ± 11.0 a.u.) versus MS with spinal cord lesions (368.0 ± 8.0 a.u., $p < 0.0001$) and versus MS without spinal cord lesions (387.3 ± 21.9 a.u., $p < 0.0001$), whereas differences between MS patients with and without spinal cord lesions were not significant ($p = 0.45$; Figure 4).

Apparent T2 Relaxation Time

Differences of T2$_{app}$ between MS patients and controls was highly significant ($p < 0.0001$ for both nerves), with higher T2$_{app}$ in controls (tibial nerve: 82.0 ± 2.1 milliseconds, peroneal nerve: 78.3 ± 1.7 milliseconds) compared to MS patients (tibial nerve: 64.3 ± 1.0 milliseconds, peroneal nerve: 61.2 ± 0.9 milliseconds; Figure 3).

TABLE . Demographic, Clinical, Radiological, and Electrophysiological Data			
Parameter	MS Patients	Controls	*p*
Age, yr	32.1 ± 1.0	31.6 ± 1.3	0.25, ns
Sex, M/F	15/21	16/19	n.a.
Body weight, kg	73.6 ± 3.0	66.2 ± 1.5	0.10, ns
Height, cm	179.1 ± 3.6	175.9 ± 2.2	0.49, ns
MS duration, mo	81.9 ± 7.3	n.a.	n.a.
Relapsing–remitting MS	34	n.a.	n.a.
Clinically isolated syndrome	2	n.a.	n.a.
Tibial nerve caliber, mm^2	52.4 ± 2.1	45.2 ± 1.4	0.0015[a]
Peroneal nerve caliber, mm^2	25.4 ± 1.3	21.3 ± 0.7	0.0049[a]
Total sciatic nerve T2w lesion number	152.7 ± 4.1	19.3 ± 1.7	<0.0001[b]
ρ tibial nerve	371.8 ± 7.7	266.0 ± 11.0	<0.0001[b]
ρ peroneal nerve	368.9 ± 8.2	276.8 ± 9.7	<0.0001[b]
Total CNS T2w lesions	27.9 ± 3.9	n.a.	n.a.
Cerebral T2w lesions	25.9 ± 3.7	n.a.	n.a.
Spinal T2w lesions	2.0 ± 0.4	n.a.	n.a.
CNS lesions with contrast enhancement	3	n.a.	n.a.
Tibial nerve CMAP, mV	21.1 ± 1.4	n.a.	n.a.
Tibial nerve NCV, m/s	54 ± 1	n.a.	n.a.
Tibial nerve F wave, ms	48.9 ± 0.6	n.a.	n.a.
Tibial nerve DML, ms	3.6 ± 0.1	n.a.	n.a.
Peroneal nerve CMAP, mV	7.7 ± 0.8	n.a.	n.a.
Peroneal nerve NCV, m/s	50 ± 1	n.a.	n.a.
Peroneal nerve F wave, ms	46.2 ± 0.7	n.a.	n.a.
Peroneal nerve DML, ms	3.7 ± 0.1	n.a.	n.a.
Sural nerve SNAP, μV	14.0 ± 1.4	n.a.	n.a.
Sural nerve NCV, m/s	57 ± 1	n.a.	n.a.

[a]Significant.
[b]Highly significant.
CMAP = compound muscle action potential; CNS = central nervous system; DML = distal motor latency; F = female; M = male; MS = multiple sclerosis; n.a. = not applicable; NCV = nerve conduction velocity; ns = not significant; SNAP = sensory nerve action potential; T2w = T2-weighted.

Nerve T2w Signal

Proximal tibial and peroneal nerve T2w signal was not significantly different between MS patients (tibial nerve: 218.5 ± 6.3 a.u., peroneal nerve: 157.6 ± 4.6 a.u.) and controls (tibial nerve: 210.6 ± 7.5 a.u., $p = 0.40$; peroneal nerve: 148.3 ± 4.6 a.u., $p = 0.12$). T2w signal of the distal tibial nerve was also not significantly different between MS patients (148.3 ± 5.1 a.u.) and controls (153.8 ± 6.5 a.u., $p = 0.55$). A significantly higher tibial nerve T2w signal could be observed at thigh level versus lower leg level in MS as well as in controls ($p < 0.0001$).

Morphometric Quantification: Nerve Diameter

Differences in proximal nerve caliber (measured as mean cross-sectional area) between MS patients and controls were significant at the level of the lumbosacral plexus

and spinal nerves (MS group: lumbosacral plexus $90.6 \pm 4.8mm^2$, spinal nerve L5 $47.6 \pm 1.9mm^2$, spinal nerve S1 $47.8 \pm 2.0mm^2$; control group: lumbosacral plexus $34.3 \pm 1.5mm^2$, spinal nerve L5 $16.4 \pm 0.6mm^2$, spinal

nerve S1 $13.2 \pm 0.6mm^2$; $p < 0.0001$ for all locations). Differences in proximal nerve caliber were also significant for the tibial nerve (MS group $52.4 \pm 2.1mm^2$, controls $45.2 \pm 1.4mm^2$, $p = 0.0015$) and the peroneal nerve (MS group $25.4 \pm 1.3mm^2$, controls $21.3 \pm 0.7mm^2$, $p = 0.0049$). However, distally, at lower leg level, there was no significant difference of tibial nerve caliber between MS patients ($34.2 \pm 1.8mm^2$) and controls ($32.1 \pm 0.9mm^2$, $p = 0.35$).

Discussion

To date, it is widely accepted that pathological changes in MS are restricted to the CNS and cranial nerves. This is reflected by the revised 2010 McDonald criteria, which only consider cerebral or spinal cord inflammatory lesions. Moreover, electrophysiological tests are commonly negative for signs of PNS involvement in MS. However, in many patients suffering from MS, there is a large, yet inexplicable gap between the severity of clinical symptoms and a comparably low burden of CNS lesions.[15,16] A few studies have indicated that damage might occur in parts of the PNS as well,[5,7,17,18] but to date, there is no solid proof of a distinct PNS affection in vivo.

To the best of our knowledge, our study is the first to prove an involvement of the PNS in MS patients by high-resolution MRN regardless of disease duration or medical treatment. Similar to the established diagnostic evaluation of T2w-hyperintense lesions in the brain and spinal cord, lesion number of the PNS can be determined visually by counting single T2w-hyperintense fascicles within lower extremity peripheral nerves with high inter-rater reliability (see Figs 1 and 2). Further signal quantification revealed a highly significant increase of ρ in MS patients compared to healthy controls, whereas $T2_{app}$ was significantly lower in the MS cohort (see Fig 3). Both ρ and $T2_{app}$ contribute to the T2w signal. However, as defined by the T2 decay, which can be calculated according to the formula $S(TE) = \rho * \exp(-TE/T2_{app})$, where S = signal and TE = echo time, an overall T2w signal increase is possible when there is an increase in ρ or $T2_{app}$, or the increase of 1 of the 2 parameters

FIGURE 1: Magnetic resonance neurography (MRN) source images. Representative MRN of the left sciatic nerve is shown at midthigh level (high-resolution T2-weighted [T2w] turbo spin echo sequence with spectral fat saturation, 3T) in (A) a healthy control subject, (B) a patient with multiple sclerosis (MS) without disease-modifying treatment, and (C) an MS patient under disease-modifying treatment. A high lesion number, measured as a marked T2w hyperintensity in a multitude of sciatic nerve fascicles, can be seen in MS patients without (B) and with (C) disease-modifying treatment. Normal sciatic nerve T2w signal in a representative healthy control is shown in A.
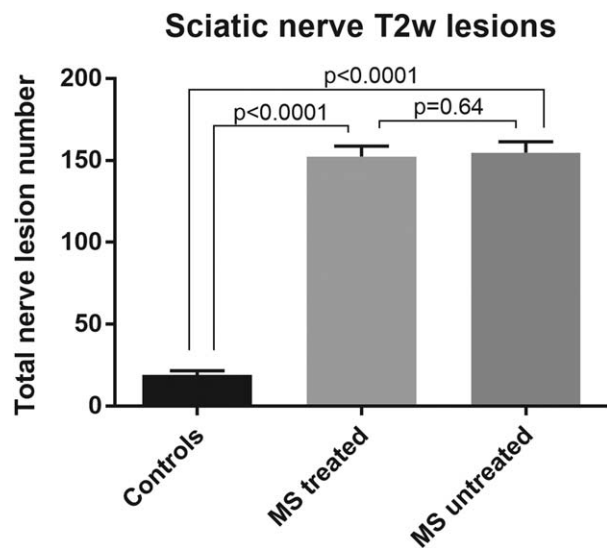
Sciatic nerve T2w lesions

FIGURE 2: Total sciatic nerve T2-weighted (T2w) lesion count. Mean values of the visually evaluated total nerve lesion number plotted for multiple sclerosis (MS) patients under immunomodulatory therapy (MS treated), MS patients without any current or previous immunomodulatory therapy (MS untreated), and controls. Whereas differences between treated and untreated MS patients were not significant ($p = 0.64$), differences between controls and each of the 2 MS subgroups were highly significant ($p < 0.0001$).

outweighs the decrease of the other. In our study cohort, the observed visual increase of fascicular T2w signal was mainly generated by an increase of ρ, which according to the T2 decay formula, outweighed the decrease of $T2_{app}$ with regard to the signal in the T2w sequence.

The subsequent classification of PNS lesions as areas of elevated ρ and slightly reduced $T2_{app}$ suggests that an increase in free-water protons, as one would expect in endoneural edema, is not the main underlying pathomechanism of PNS involvement in MS.[19,20] Instead, an increasing ρ indicates that damage to the PNS in MS is more likely induced by changes in the microstructural organization of the extracellular matrix as a consequence of an increase in plasma protein leakage through the endovascular barrier, and the pathogenesis of a proinflammatory milieu.[21] This mechanism was previously hypothesized as key factor in the pathomechanism of typical PNS diseases such as amyloidotic or diabetic neuropathy.[12,13] Additionally, previous MRI studies focusing on changes of ρ in CNS lesions related to MS found a clear correlation between an increased ρ and areas of demyelination in the brain and spinal cord,[22] suggesting that our findings represent a peripheral codemyelination of the PNS in MS. Thus, an increase in ρ supports the assumption that PNS lesions or rather a peripheral codemyelination is likely to be caused by immunologic reactions and destruction of molecules such as connexin 32 or myelin-associated glycoproteins that are common to myelinating cells in both the PNS and the CNS.[23–25]

Alterations of $T2_{app}$ in MS are still not fully understood.[26] Previous studies described an initial increase of $T2_{app}$ in acute MS lesions with a subsequent decrease in chronic lesions, but results are controversial.[27–30] One possible explanation might be a balance change of the total water pool toward a higher amount of bound water and a lower amount of free water molecules, as would be the case in the suggested hypotheses of an inflammatory process combined with an impairment of the blood–nerve barrier, a pathologically high plasma protein leakage, and an impairment of the lipid-rich myelin sheath.[1,21]

Peripheral nerve lesion detection by means of the described qualitative and quantitative analysis of the magnetic resonance signal was further validated by an additional increase of proximal tibial and peroneal nerve caliber in MS, representing a pure morphometric MRN criterion for nerve impairment. This proximal nerve caliber increase might also point toward an inflammatory process, especially as it was associated with a higher number of PNS lesions and an increased ρ. However, differences between MS patients and healthy controls were insignificant for distal tibial nerve caliber, suggesting a proximal predominance of PNS affection.

This study is limited in that most enrolled patients were under disease-modifying treatment. An argument could be made that lesions are attributed to secondary effects of MS modifying medications rather than to the disease itself. To the contrary, we found no difference in the lesion number of patients with and without medication. Furthermore, MS patients were treated with a multitude of different immunomodulating drugs, of which none has known acute or chronic neurotoxic side effects. One might also argue that, in comparison to controversial results in previous studies, but also in the absence of positive electrophysiological examination results, our finding of an elevated number of PNS lesions in all included patients seems improbable. An explanation might be that PNS involvement is very subtle in many cases and thus may escape detection by regular nerve conduction velocity examinations, as in our study. However, recent studies focusing on demyelinating processes in corneal fibers of the trigeminal nerve have shown that PNS demyelination is present in more patients than clinical symptoms might suggest.[31] Both corneal fiber microscopy and MRN have already shown that damage to PNS fibers is detectable prior to the beginning of clinical symptoms.[12,31,32]

A potential factor that might contribute to the occurrence of PNS lesions is that PNS lesions are the result of Wallerian degeneration caused by spinal cord lesions in MS.[9] Although we cannot fully exclude such secondary effects of CNS lesions, we found no differences in MRN markers between patients with and without spinal cord
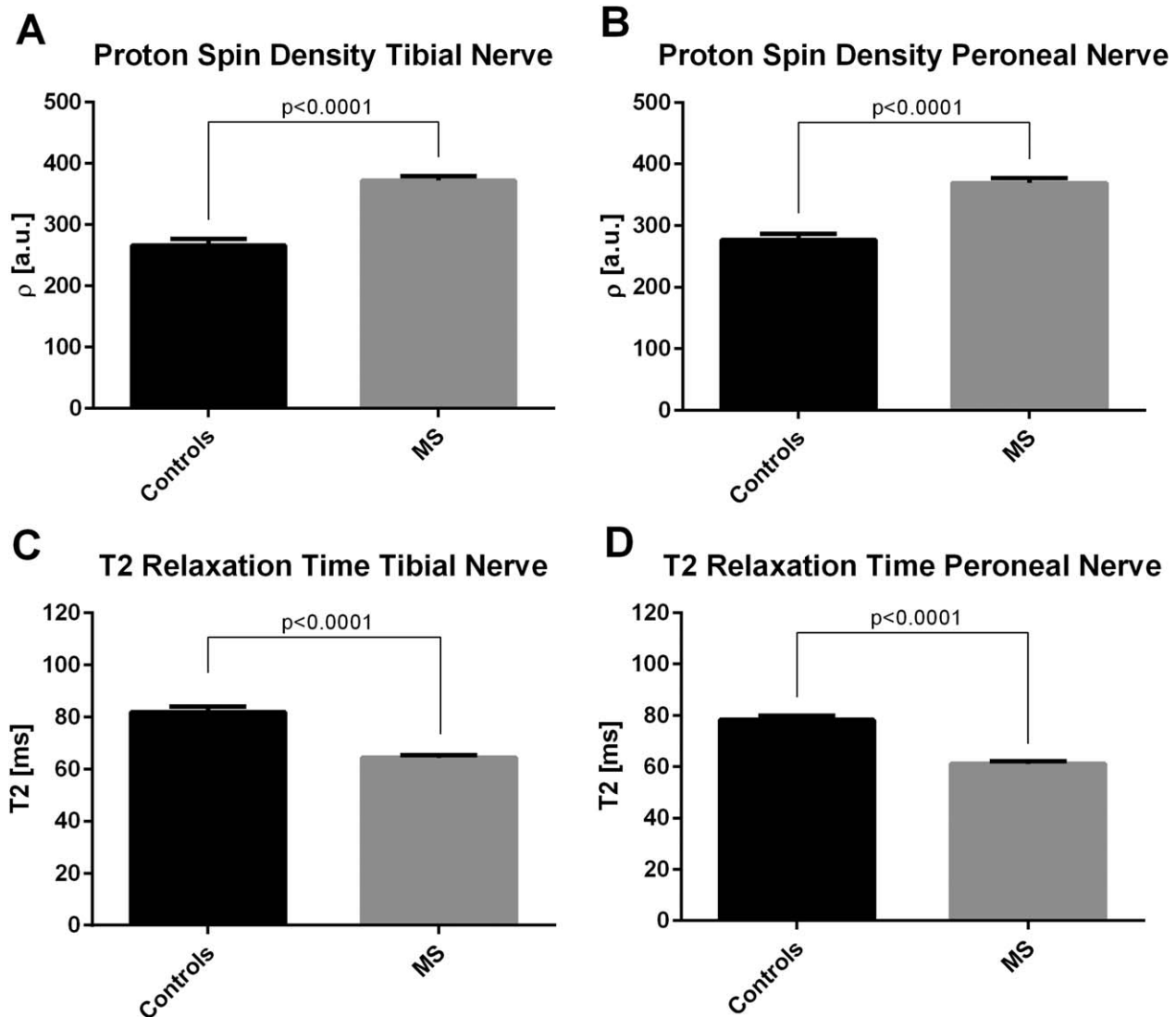
FIGURE 3: Quantitative magnetic resonance neurography markers of nerve T2-weighted signal. Mean values of tibial (left) and peroneal (right) proton spin density (A, B) and apparent T2 relaxation time (C, D) are plotted for multiple sclerosis (MS) patients and controls. Proton spin density of the tibial (A) and peroneal nerve (B) was significantly higher in MS patients versus healthy controls ($p < 0.0001$). In contrast, tibial (C) and peroneal nerve (D) apparent T2 relaxation time was significantly higher in controls versus MS patients ($p < 0.0001$). a.u. = arbitrary units.

lesions (Fig 4). The finding of a negative correlation between PNS lesions and spinal cord lesions and also the exclusion of any other potential sources of CNS damage in the additionally available spinal MRIs make it even more unlikely that the observed PNS lesions occur as a direct consequence of spinal cord lesions. Furthermore, the diffuse, nonfocal PNS lesion distribution in our study cohort, which involved only short continuous fascicular segments, points more toward an underlying inflammatory or demyelinating pathomechanism as one would expect in MS. In contrast, an involvement of longer fascicular segments or a somatotopic fascicular organization, as has been demonstrated in Wallerian degeneration,[33–36] could be excluded. Electrophysiological examinations also revealed no abnormalities due to an axonal loss, as they

typically occur in Wallerian degeneration. For all these reasons, our study results indicate a potential occurrence of different antibodies in MS with and without CNS predominance.

Future studies should point at differences in patients with MS and clinically isolated syndrome with and without PNS lesions. Special attention should be paid to individuals with a relatively low CNS lesion burden in comparison to severe clinical symptoms, and to the influence of different disease-modifying drugs on the development of PNS lesions.

In summary, this proof-of-concept study evidences PNS lesions in young MS patients in vivo by MRN with high structural resolution. The identification of PNS lesions suggests a peripheral codemyelination, which may
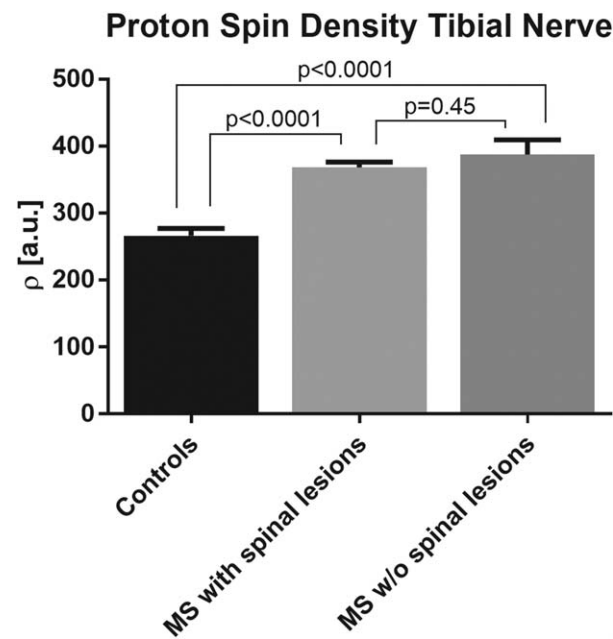
Proton Spin Density Tibial Nerve

FIGURE 4: Proton spin density. Mean values of tibial nerve proton spin density are plotted for multiple sclerosis (MS) patients with and without spinal cord T2-weighted (T2w) lesions and for controls. Note that differences in proton spin density between MS patients with and without T2w lesions to the spinal cord were not significant ($p = 0.45$), whereas differences between controls and either MS subgroup were remarkable ($p < 0.0001$).

guide to a better understanding of discrepancies between clinical symptoms and CNS lesions detected by MRI. Most importantly, it provides options for new pathophysiological concepts, and the identification of potential distinct immunoreactions targeting PNS antigens in MS with future implications for therapeutic approaches.

Acknowledgment

Author Contributions

J.K., G.H.H., J.M.E.J., J.P., M.P., and M.B. conceived and designed the study. J.K., G.H.H., J.M.E.J., R.D., M.W., S.H., B.W., M.K.-K., and J.M.H. acquired and analyzed data. J.K., G.H.H., J.M.E.J., W.W., and M.B. were responsible for writing and drafting a significant portion of the manuscript or figures.

Potential Conflicts of Interest

Nothing to report.

References

1. Kister I, Bacon TE, Chamot E, et al. Natural history of multiple sclerosis symptoms. Int J MS Care 2013;15:146–158.

2. Poser CM, Paty DW, Scheinberg L, et al. New diagnostic criteria for multiple sclerosis: guidelines for research protocols. Ann Neurol 1983;13:227–231.

3. Polman CH, Reingold SC, Banwell B, et al. Diagnostic criteria for multiple sclerosis: 2010 revisions to the McDonald criteria. Ann Neurol 2011;69:292–302.

4. Hasson J, Terry RD, Zimmerman HM. Peripheral neuropathy in multiple sclerosis. Neurology 1958;8:503–510.

5. Pollock M, Calder C, Allpress S. Peripheral nerve abnormality in multiple sclerosis. Ann Neurol 1977;2:41–48.

6. Vogt J, Paul F, Aktas O, et al. Lower motor neuron loss in multiple sclerosis and experimental autoimmune encephalomyelitis. Ann Neurol 2009;66:310–322.

7. Anlar O, Tombul T, Kisli M. Peripheral sensory and motor abnormalities in patients with multiple sclerosis. Electromyogr Clin Neurophysiol 2003;43:349–351.

8. Stoll G, Bendszus M, Perez J, Pham M. Magnetic resonance imaging of the peripheral nervous system. J Neurol 2009;256:1043–1051.

9. Bendszus M, Stoll G. Technology insight: visualizing peripheral nerve injury using MRI. Nat Clin Pract Neurol 2005;1:45–53.

10. Kurtzke JF. Rating neurologic impairment in multiple sclerosis: an expanded disability status scale (EDSS). Neurology 1983;33:1444–1452.

11. Jenkinson M, Beckmann CF, Behrens TEJ, et al. FSL. Neuroimage 2012;62:782–790.

12. Kollmer J, Hund E, Hornung B, et al. In vivo detection of nerve injury in familial amyloid polyneuropathy by magnetic resonance neurography. Brain 2015;138:549–562.

13. Pham M, Oikonomou D, Hornung B, et al. Magnetic resonance neurography detects diabetic neuropathy early and with proximal predominance. Ann Neurol 2015;78:939–948.

14. Heiland S, Sartor K, Martin E, et al. In vivo monitoring of age-related changes in rat brain using quantitative diffusion magnetic resonance imaging and magnetic resonance relaxometry. Neurosci Lett 2002;334:157–160.

15. Rovaris M, Bozzali M, Santuccio G, et al. In vivo assessment of the brain and cervical cord pathology of patients with primary progressive multiple sclerosis. Brain 2001;124(pt 12):2540–2549.

16. Miller DH, Grossman RI, Reingold SC, McFarland HF. The role of magnetic resonance techniques in understanding and managing multiple sclerosis. Brain 1998;121(pt 1):3–24.

17. Schoene WC, Carpenter S, Behan PO, Geschwind N. "Onion bulb" formations in the central and peripheral nervous system in

association with multiple sclerosis and hypertrophic polyneuropathy. Brain 1977;100:755–773.

18. Misawa S, Kuwabara S, Mori M, et al. Peripheral nerve demyelination in multiple sclerosis. Clin Neurophysiol 2008;119:1829–1833.

19. Abbas Z, Gras V, Möllenhoff K, et al. Analysis of proton-density bias corrections based on T_1 measurement for robust quantification of water content in the brain at 3 Tesla. Magn Reson Med 2014;72:1735–1745.

20. Tofts PS, du Boulay EP. Towards quantitative measurements of relaxation times and other parameters in the brain. Neuroradiology 1990;32:407–415.

21. Davies G, Ramani A, Dalton C, et al. Preliminary magnetic resonance study of the macromolecular proton fraction in white matter: a potential marker of myelin? Mult Scler 2003;9:246–249.

22. Nijeholt GJ, Bergers E, Kamphorst W, et al. Post-mortem high-resolution MRI of the spinal cord in multiple sclerosis: a correlative study with conventional MRI, histopathology and clinical phenotype. Brain 2001;124(pt 1):154–166.

23. Pichiecchio A, Bergamaschi R, Tavazzi E, et al. Bilateral trigeminal enhancement on magnetic resonance imaging in a patient with multiple sclerosis and trigeminal neuralgia. Mult Scler 2007;13:814–816.

24. Gartzen K, Katzarava Z, Diener H-C, Putzki N. Peripheral nervous system involvement in multiple sclerosis. Eur J Neurol 2011;18:789–791.

25. Rovira A. Peripheral nervous system involvement in multiple sclerosis. Mult Scler 2017;23:751.

26. MacKay AL, Laule C. Magnetic resonance of myelin water: an in vivo marker for myelin. Brain Plast 2016;2:71–91.

27. Ormerod I, Bronstein A, Rudge P, et al. Magnetic resonance imaging in clinically isolated lesions of the brain stem. J Neurol Neurosurg Psychiatry 1986;49:737–743.

28. Goodkin DE, Rooney WD, Sloan R, et al. A serial study of new MS lesions and the white matter from which they arise. Neurology 1998;51:1689–1697.

29. Larsson HB, Frederiksen J, Petersen J, et al. Assessment of demyelination, edema, and gliosis by in vivo determination of T1 and T2 in the brain of patients with acute attack of multiple sclerosis. Magn Reson Med 1989;11:337–348.

30. Deoni SCL. Quantitative relaxometry of the brain. Top Magn Reson Imaging 2010;21:101–113.

31. Mikolajczak J, Zimmermann H, Kheirkhah A, et al. Patients with multiple sclerosis demonstrate reduced subbasal corneal nerve fibre density. Mult Scler 2016 Nov 1, epub ahead of print

32. Kollmer J, Sahm F, Hegenbart U, et al. Sural nerve injury in familial amyloid polyneuropathy: MR neurography vs clinicopathologic tools. Neurology 2017;89:475–484.

33. Baumer P, Weiler M, Bendszus M, Pham M. Somatotopic fascicular organization of the human sciatic nerve demonstrated by MR neurography. Neurology 2015;84:1782–1787.

34. Hilgenfeld T, Jende J, Schwarz D, et al. Somatotopic fascicular lesions of the brachial plexus demonstrated by high-resolution magnetic resonance neurography. Invest Radiol 2017 Jul 18, epub ahead of print

35. Bendszus M, Wessig C, Solymosi L, et al. MRI of peripheral nerve degeneration and regeneration: correlation with electrophysiology and histology. Exp Neurol 2004;188:171–177.

36. Stanisz GJ, Midha R, Munro CA, Henkelman RM. MR properties of rat sciatic nerve following trauma. Magn Reson Med 2001;45:415–420.